Supporting Information for

Crystallographic Characterization of $Ti_2C_2@D_{3h}(5)$-C_{78}, $Ti_2C_2@C_{3v}(8)$-C_{82}, and $Ti_2C_2@C_s(6)$-C_{82}: Identification of Unsupported Ti_2C_2 Cluster with Cage-dependent Configurations

Pengyuan Yu,[a] Lipiao Bao,[a] Le Yang,[b] Debo Hao,[b] Peng Jin,*[b] Wangqiang Shen,*[a] Hongyun Fang,*[a] Takeshi Akasaka[a] and Xing Lu*[a]

[a] *State Key Laboratory of Materials Processing and Die & Mould Technology, School of Materials Science and Engineering, Huazhong University of Science and Technology, 1037 Luoyu Road, Wuhan, 430074 China.*

E-mail: lux@hust.edu.cn

[b] *School of Materials Science and Engineering, Hebei University of Technology, Tianjin, 300130 China.*

E-mail: china.peng.jin@gmail.com

Contents

Table S1. Occupancy values of the two Ti atoms inside the Ti_2C_2@D_{3h}(5)-C_{78}, Ti_2C_2@C_s(6)-C_{82}, and Ti_2C_2@C_{3v}(8)-C_{82}.

Table S2. Structural parameters of Ti_2C_2 cluster inside the Ti_2C_2@D_{3h}(5)-C_{78}, Ti_2C_2@C_s(6)-C_{82}, and Ti_2C_2@C_{3v}(8)-C_{82}.

Table S3. Vis-NIR absorptions of Ti_2C_2@D_{3h}(5)-C_{78} and related C_{78}-based EMFs.

Table S4. Vis-NIR absorptions of Ti_2C_2@C_s(6)-C_{82}, Ti_2C_2@C_{3v}(8)-C_{82}, and related C_{82}-based EMFs.

Figure S4. CV curves of Ti_2C_2@C_s(6)-C_{82} and Ti_2C_2@C_{3v}(8)-C_{82}.

Figure S5. Optimized structures, symmetries and relative energies (kcal/mol) of different isomers of Ti_2C_2@D_{3h}(5)-C_{78}, Ti_2C_2@C_s(6)-C_{82}, and Ti_2C_2@C_{3v}(8)-C_{82} at the M06-2X/6-31G*~SDD level of theory.

Reference

General information

General characterization.

HPLC was conducted on an LC-908 machine (Japan Analytical Industry Co., Ltd.). The positive-ion mode matrix-assisted laser desorption/ionization time-of-flight (MALDI-TOF) (MICROFLEX, Bruker, Germany) was used for the mass spectroscopic characterization. The Vis-NIR spectra were measured by a PE Lambda 750S spectrophotometer in carbon disulfide. Cyclic voltammogram was measured in *o*-DCB with 0.05M $TBAPF_6$ as the supporting electrolyte with a CHI660E workstation.

Crystallographic characterizations.

Single-crystal X-ray data were collected at 100 K using the radiation wavelength at 0.7749 (for Ti_2C_2@C_{78}) or 0.8264 Å (for Ti_2C_2@C_{82} isomers) with a MarCCD detector at beamline BL17B of the Shanghai Synchrotron Radiation Facility (China). A multi-scan method (SADABS) was used for absorption corrections. The structures were solved with direct methods and were refined with SHELXL-2014.[S1]

Computational Methods

Full geometry optimizations were carried out by using the M06-2X functional[S2] and the standard 6-31G* all-electron basis set for C[S3] and the Stuttgart/Dresden relativistic effective core potential[S4] and corresponding basis set for Ti. All the DFT calculations were performed by using the Gaussian 09 software package.[S5]

Synthesis and isolation of Ti_2C_2@$\boldsymbol{D_{3h}}$(5)-C_{78}, Ti_2C_2@$\boldsymbol{C_s}$(6)-C_{82} and Ti_2C_2@$\boldsymbol{C_{3v}}$(8)-C_{82}.

Soot containing titanium metallofullerenes was produced with the arc-discharge method. Specifically, graphite rods containing a mixture of TiC and graphite powder (molar ratio: Ti/C=1:10) were vaporized under 400 mbar He atmosphere. The crude mixture of empty fullerenes and titanium-containing EMFs was extracted with carbon disulfide. Lewis acid $SnCl_4$ was chosen to react with the extract for the enrichment of Ti-EMFs. Then the precipitate was collected. After filtration, decomplexation of the precipitate occurred with the treatment of deionized water. The resulting solid was dissolved in carbon disulfide. Upon solvent removal, the sample was re-dissolved in chlorobenzene for multiple HPLC separations. (vide infra).

HPLC separation of Ti_2C_2@$\boldsymbol{D_{3h}}$(5)-C_{78}, Ti_2C_2@$\boldsymbol{C_s}$(6)-C_{82} and Ti_2C_2@$\boldsymbol{C_{3v}}$(8)-C_{82}

The precipitation (named **Fo**) obtained by $SnCl_4$ treatment was re-dissolved in chlorobenzene and isolated by two-stage HPLC separations. In the first stage, **Fo** was separated on a 5PBB column (20 mm × 250 mm, Cosmosil Nacalai Tesque) with chlorobenzene as mobile phase. Then two fractions of **Fo-5** and **Fo-7** were collected for the final stage of separation on Buckyprep-M column (10mm × 250mm) and Buckyprep column (10mm × 250mm) with toluene as mobile phase, respectively. Finally, pure Ti_2C_{80} and Ti_2C_2@C_{82}(I, II) were collected named **Fo-5-3**, **Fo-7-6,** and **Fo-7-7**, respectively.

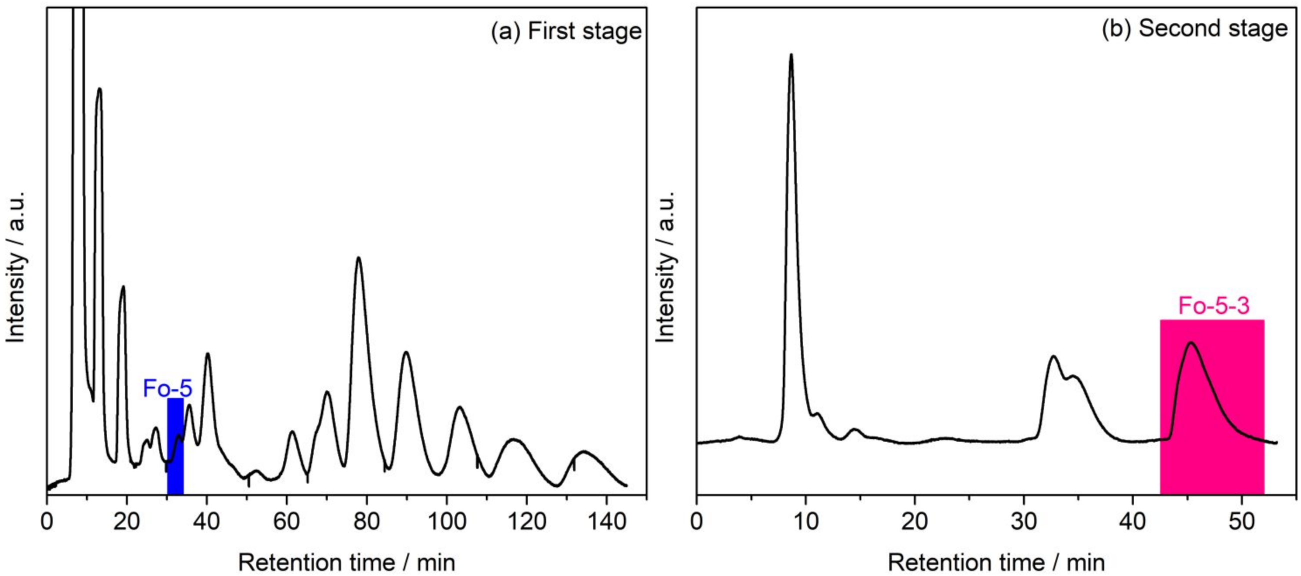

Figure S1. Isolation schemes of Ti_2C_{80}. (a) The first stage HPLC chromatogram of **Fo** dissolved in chlorobenzene. Conditions: 5PBB column, Φ = 20 mm × 250 mm, eluent = chlorobenzene, flow rate = 10 mL/min, detection wavelength = 330 nm, room temperature. (b) The second stage HPLC chromatogram of fraction **Fo-5**. Conditions: Buckyprep-M column, Φ = 20 mm × 250 mm, eluent = toluene, flow rate = 4 mL/min, detection wavelength = 330 nm, room temperature.

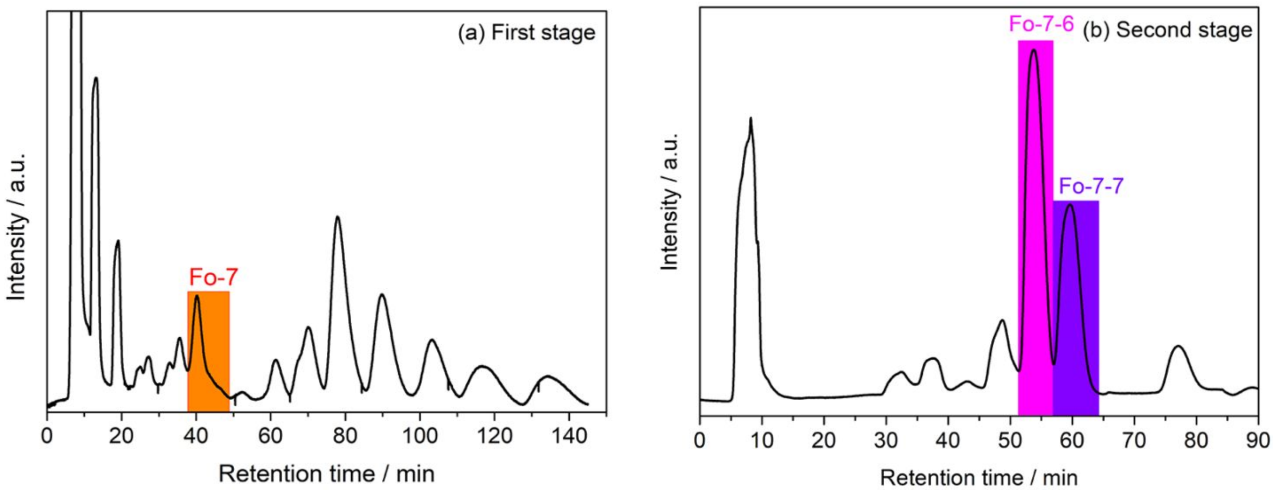

Figure S2. Isolation schemes of Ti_2C_{84}(I) and Ti_2C_{84}(II). (a) The first stage HPLC chromatogram of **Fo** dissolved in chlorobenzene. Conditions: 5PBB column, Φ = 20 mm × 250 mm, eluent = chlorobenzene, flow rate = 10 mL/min, detection wavelength = 330 nm, room temperature. (b) The second stage HPLC chromatogram of fraction **Fo-7**. Conditions: Buckyprep column, Φ = 10 mm × 250 mm, eluent = toluene, flow rate = 4 mL/min, detection wavelength = 330 nm, room temperature.

Crystal data of Ti_2C_2@D_{3h}(5)-C_{78}·Ni(OEP)·2(C_7H_8). black block, 0.20 × 0.10 × 0.10 mm, monoclinic, space group $P2_1/c$, a = 20.364(4) Å, b = 14.740(3) Å, c = 25.377(5) Å, α= 90°, β = 98.02(3)°, γ = 90°, V = 7543(3) Å^3, Fw = 1832.33, λ = 0.7749 Å, Z = 4, D_{calc} = 1.614 Mg/m^3, μ = 0.658 mm^{-1}, T = 100 K, R_1 = 0.0847, wR_2 = 0.2607, GOF (on F^2) = 1.037. The maximum residual electron density is 0.844 eÅ^{-3}. Crystallographic data has been deposited in the Cambridge Crystallographic Data Center with the CCDC number 1951586.

Crystal data of Ti_2C_2@C_s(6)-C_{82}·Ni(OEP)·2(C_7H_8). black block, 0.30 × 0.23 × 0.18 mm, monoclinic, space group $C2/m$, a = 25.3093(9) Å, b = 14.8746(6) Å, c = 20.5507(7) Å, α= 90°, β = 96.880(2)°, γ = 90°, V = 7680.9(5) Å^3, Fw = 1880.37, λ = 0.8264 Å, Z = 4, D_{calc} = 1.626 Mg/m^3, μ = 0.772 mm^{-1}, T = 100 K, R_1 = 0.0799, wR_2 = 0.1829, GOF (on F^2) = 1.142. The maximum residual electron density is 0.681 eÅ^{-3}. Crystallographic data has been deposited in the Cambridge Crystallographic Data Center with the CCDC number 1892499.

Crystal data of Ti_2C_2@C_{3v}(8)-C_{82}·Ni(OEP)·2(C_7H_8). black block, 0.28 × 0.20× 0.12 mm, monoclinic, space group $C2/m$, a = 25.3264(10) Å, b = 14.9476(7) Å, c =20.4238(9) Å, α= 90°, β = 97.621(2)°, γ = 90°, V = 7663.5(6) Å^3, Fw = 1880.37, λ = 0.8264 Å, Z = 4, D_{calc} = 1.630 Mg/m^3, μ = 0.773 mm^{-1}, T = 100 K, R_1 = 0.1158, wR_2 = 0.2846, GOF (on F^2) = 1.148. The maximum residual electron density is 1.060 eÅ^{-3}. Crystallographic data has been deposited in the Cambridge Crystallographic Data Center with the CCDC number 1892500.

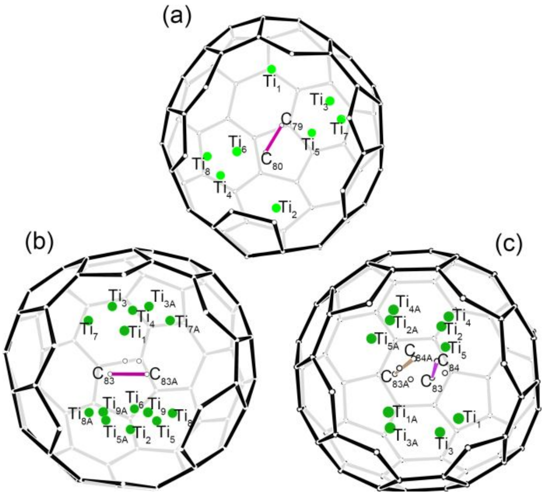

Figure S3. Perspective drawings showing the disordered titanium sites in (a) $Ti_2C_2@D_{3h}(5)-C_{78}$, (b) $Ti_2C_2@C_s(6)-C_{82}$, and (c) $Ti_2C_2@C_{3v}(8)-C_{82}$. The atoms labeled with ‘A’ are generated by the crystallographic operation. Some cage frameworks are omitted to enhance visualization.

Inside the fullerene cages, the titanium atoms show some degree of disorder and the number of the disordered titanium sites increases as the cage size expands (from C_{78} to C_{82}). In detail, 8, 14, and 10 titanium positions are found for the two Ti atoms in $D_{3h}(5)-C_{78}$, $C_s(6)-C_{82}$, and $C_{3v}(8)-C_{82}$, respectively, indicating the motional behavior for the titanium atoms inside the fullerene cages.

Table S1. Occupancy values of the two Ti atoms inside $Ti_2C_2@D_{3h}(5)-C_{78}$, $Ti_2C_2@C_s(6)-C_{82}$, and $Ti_2C_2@C_{3v}(8)-C_{82}$.[a]

EMFs	Occupancy values of Ti atoms								
$Ti_2C_2@D_{3h}(5)-C_{78}$	Ti1	Ti2	Ti3	Ti4	Ti5	Ti6	Ti7	Ti8	-
	0.62	0.62	0.22	0.22	0.11	0.11	0.05	0.05	-
$Ti_2C_2@C_s(6)-C_{82}$	Ti1	Ti2	Ti3/ Ti3A	Ti4	Ti5/ Ti5A	Ti6	Ti7/ Ti7A	Ti8/ Ti8A	Ti9/ Ti9A
	0.56	0.24	0.07	0.07	0.20	0.11	0.11	0.07	0.05

$Ti_2C_2@C_{3v}(8)$-C_{82}	Ti1/ Ti1A	Ti2/ Ti2A	Ti3/ Ti3A	Ti4/ Ti4A	Ti5/ Ti5A	-	-	-	-
	0.29	0.34	0.21	0.10	0.06	-	-	-	-

[a] Atoms labeled 'A' are generated by the crystallographic mirror plane.

Table S2. Ti-cage distances and structural parameters of the Ti_2C_2 clusters of $Ti_2C_2@D_{3h}(5)$-C_{78}, $Ti_2C_2@C_s(6)$-C_{82}, and $Ti_2C_2@C_{3v}(8)$-C_{82}.[a]

EMF	Ti···Ti distance (Å)	Ti-C distances (Å)	C-C distance (Å)	Ti-cage distances (Å)	Ti-C_2-Ti dihedral angle
$Ti_2C_2@D_{3h}(5)$-C_{78}	5.000	2.054-2.065	1.115	2.086-2.252	176.87°
$Ti_2C_2@C_s(6)$-C_{82}	3.860	2.039-2.086	1.207	2.078-2.128	147.52°
$Ti_2C_2@C_{3v}(8)$-C_{82}	3.633	1.866-2.082	1.300	2.065-2.236	156.35°

[a] The prominent Ti_2C_2 cluster and fullerene cage in these EMFs.

Table S3. Details of the Vis-NIR absorptions of $Ti_2C_2@D_{3h}(5)$-C_{78} and selected $D_{3h}(5)$-C_{78}-based EMFs.

EMF	Absorption bands (nm)	Onset (nm)	Optical bandgap (eV)[a]
$Ti_2C_2@D_{3h}(5)$-C_{78}	457, 550, 612, 720, 850	1400	0.88
$Ti_2S@D_{3h}(5)$-C_{78}[S6]	498, 602, 657, 757, 896	1470	0.84
$Sc_3N@D_{3h}(5)$-C_{78}[S7]	460,623	-	-

[a] Optical bandgap (eV) ≈ 1240/onset (nm)

Table S4. Details of the Vis-NIR absorptions of Ti_2C_2@C_s(6)-C_{82}, Ti_2C_2@C_{3v}(8)-C_{82}, and selected C_{82}-based EMFs.

EMF	Absorption bands (nm)	Onset (nm)	Optical bandgap (eV)[a]
Ti_2C_2@C_s(6)-C_{82}	622,719,1050	1600	0.78
Y_2C_2@C_s(6)-C_{82}[S8]	629,715,791,858,1055,1204	1470	0.84
Sc_2O@C_s(6)-C_{82}[S9]	-[b]	1550	0.80
Sc_2S@C_s(6)-C_{82}[S10]	511, 660, 720, 758, 1178	1351	0.89
Ti_2C_2@C_{3v}(8)-C_{82}	570,737,1017	1600	0.78
Y_2C_2@C_{3v}(8)-C_{82}[S8]	570, 684, 790,880,1000	1100	1.13
Sc_2O@C_{3v}(8)-C_{82}	665,884,718-821	1090	1.14
Sc_2S@C_{3v}(8)-C_{82}[S11]	-	1240	1.00

[a] Optical bandgap (eV) ≈ 1240/onset (nm) [b] Visible range with strong absorption at 500 nm.

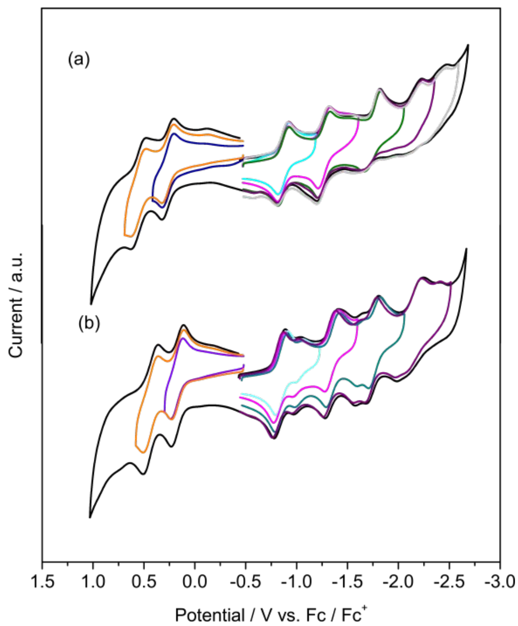

Figure S4. Cyclic voltammogram of (a) Ti_2C_2@C_{3v}(8)-C_{82} and (b) Ti_2C_2@C_s(6)-C_{82} in *o*-dichlorobenzene. (0.05 M $TBAPF_6$; scan rate 100 mv/s for CV)

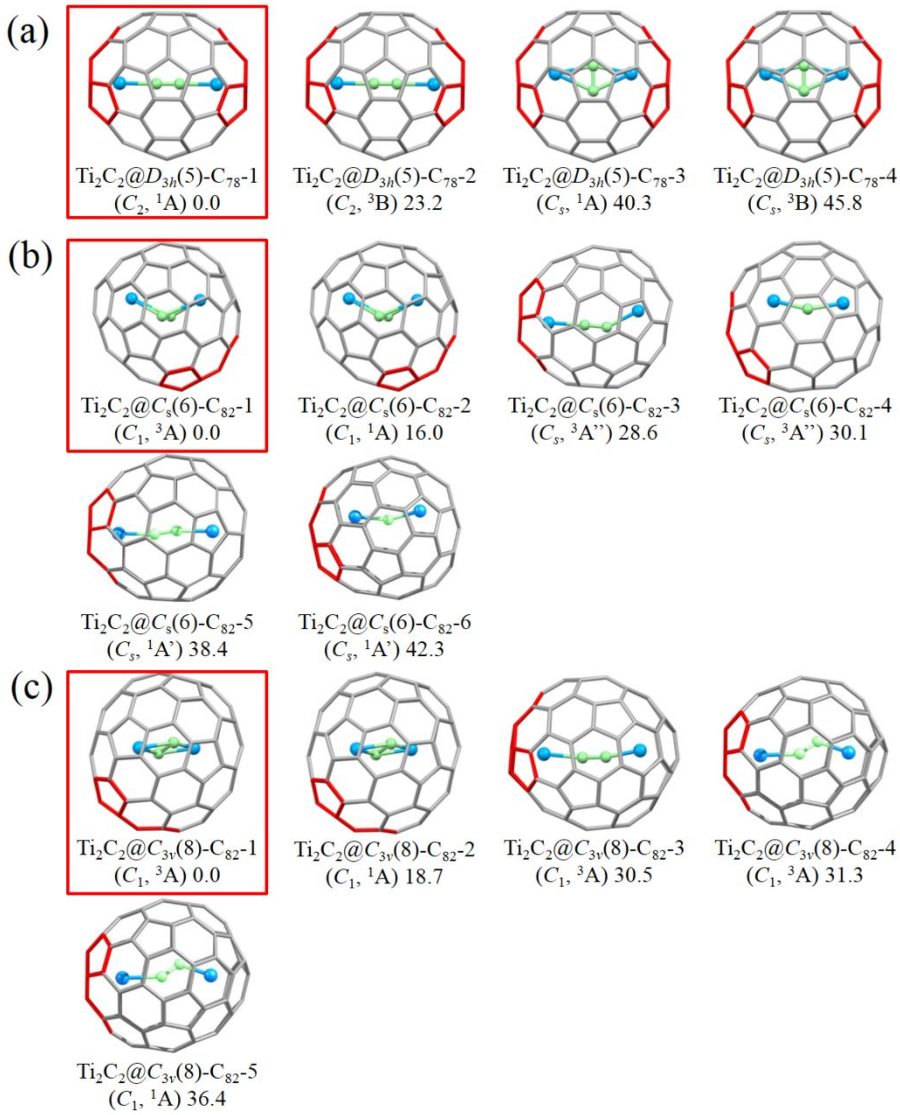

Figure S5. Optimized structures, symmetries and relative energies (kcal/mol) of different isomers of (a) $Ti_2C_2@D_{3h}(5)$-C_{78}, (b) $Ti_2C_2@C_s(6)$-C_{82}, and (c) $Ti_2C_2@C_{3v}(8)$-C_{82} at the M06-2X/6-31G*~SDD level of theory. The isomers marked with a red box are experimentally obtained. The sumanene motif(s) in the three involved EMFs are colored red.

Reference

S1 Sheldrick, G. M. A Short History of SHELX. *Acta Crystallogr. A.* **2008**, *64*, 112–122.

S2 Zhao, Y.; Truhlar, D. G. The M06 Suite of Density Functionals for Main Group Thermochemistry, Thermochemical Kinetics, Noncovalent Interactions, Excited States, and Transition Elements: Two New Functionals and Systematic Testing of Four M06-Class Functionals and 12 Other Functionals. *Theor. Chem. Account.* **2008**, *120*, 215–241.

S3 Hehre, W. J.; Ditchfield, R.; Pople, J. A. Self—Consistent Molecular Orbital Methods. XII. Further Extensions of

Gaussian—Type Basis Sets for Use in Molecular Orbital Studies of Organic Molecules. *J. Chem. Phys.* **1972**, *56*, 2257–2261.

S4 Cao, X.; Dolg, M. Segmented Contraction Scheme for Small-Core Lanthanide Pseudopotential Basis Sets. *J. Mol. Struct. THEOCHEM.* **2002**, *581*, 139–147.

S5 M. J. Frisch, G. W. Trucks, H. B. Schlegel, G. E. Scuseria, M. A. Robb, J. R. Cheeseman, G. Scalmani, V. Barone, B. Mennucci, G. A. Petersson, H. Nakatsuji, M. Caricato, X. Li, H. P. Hratchian, A. F. Izmaylov, J. Bloino, G. Zheng, J. L. Sonnenberg, M. Hada, M. Ehara, K. Toyota, R. Fukuda, J. Hasegawa, M. Ishida, T. Nakajima, Y. Honda, O. Kitao, H. Nakai, T. Vreven, J. A. Montgomery, Jr., J. E. Peralta, F. Ogliaro, M. Bearpark, J. J. Heyd, E. Brothers, K. N. Kudin, V. N. Staroverov, R. Kobayashi, J. Normand, K. Raghavachari, A. Rendell, J. C. Burant, S. S. Iyengar, J. Tomasi, M. Cossi, N. Rega, J. M. Millam, M. Klene, J. E. Knox, J. B. Cross, V. Bakken, C. Adamo, J. Jaramillo, R. Gomperts, R. E. Stratmann, O. Yazyev, A. J. Austin, R. Cammi, C. Pomelli, J. W. Ochterski, R. L. Martin, K. Morokuma, V. G. Zakrzewski, G. A. Voth, P. Salvador, J. J. Dannenberg, S. Dapprich, A. D. Daniels, Ö. Farkas, J. B. Foresman, J. V. Ortiz, J. Cioslowski and D. J. Fox, Gaussian 09, Revision E.01, Gaussian, Inc., Wallingford CT, 2013.

S6 Li, F.-F.; Chen, N.; Mulet-Gas, M.; Triana, V.; Murillo, J.; Rodríguez-Fortea, A.; Poblet, J. M.; Echegoyen, L. $Ti_2S@D_{3h}(24109)-C_{78}$: A Sulfide Cluster Metallofullerene Containing Only Transition Metals inside the Cage. *Chem. Sci.* **2013**, *4*, 3404–3410.

S7 Olmstead, M. M.; de Bettencourt-Dias, A.; Duchamp, J. C.; Stevenson, S.; Marciu, D.; Dorn, H. C.; Balch, A. L. Isolation and Structural Characterization of the Endohedral Fullerene $Sc_3N@C_{78}$. *Angew. Chem. Int. Ed.* **2001**, *40*, 1223–1225.

S8 Inoue, T.; Tomiyama, T.; Sugai, T.; Okazaki, T.; Suematsu, T.; Fujii, N.; Utsumi, H.; Nojima, K.; Shinohara, H. Trapping a C_2 Radical in Endohedral Metallofullerenes: Synthesis and Structures of $(Y_2C_2)@C_{82}$ (Isomers I, II, and III). *J. Phys. Chem. B* **2004**, *108*, 7573–7579.

S9 Mercado, B. Q.; Stuart, M. A.; Mackey, M. A.; Pickens, J. E.; Confait, B. S.; Stevenson, S.; Easterling, M. L.; Valencia, R.; Rodríguez-Fortea, A.; Poblet, J. M.; Olmstead, M. M.; Balch, A. L. $Sc_2(\mu_2\text{-O})$ Trapped in a Fullerene Cage: The

Isolation and Structural Characterization of $Sc_2(\mu_2\text{-}O)@C_s(6)\text{-}C_{82}$ and the Relevance of the Thermal and Entropic Effects in Fullerene Isomer Selection. *J. Am. Chem. Soc.* **2010**, *132*, 12098–12105.

S10 Chen, N.; Chaur, M. N.; Moore, C.; Pinzón, J. R.; Valencia, R.; Rodríguez-Fortea, A.; Poblet, J. M.; Echegoyen, L. Synthesis of a New Endohedral Fullerene Family, $Sc_2S@C_{2n}$ (n = 40–50) by the Introduction of SO_2. *Chem. Commun.* **2010**, *46*, 4818–4820.

S11 Dunsch, L.; Yang, S.; Zhang, L.; Svitova, A.; Oswald, S.; Popov, A. A. Metal Sulfide in a C_{82} Fullerene Cage: A New Form of Endohedral Clusterfullerenes. *J. Am. Chem. Soc.* **2010**, *132*, 5413–5421.